ACS OMEGA

http://pubs.acs.org/journal/acsodf

Article

Metallic Germanium (111) Slab Structures

Chih Shan Tan*

Cite This: *ACS Omega* 2023, 8, 22238−22244

Read Online

ACCESS | Metrics & More | Article Recommendations | Supporting Information

ABSTRACT: Prior research has indicated that the surface electron conductivity of Ge (111) wafers surpasses that of Ge (100) and Ge (110) wafers. This disparity has been ascribed to the variations in bond length, geometry, and frontier orbital electron energy distribution across different surface planes. The ab initio molecular dynamics (AIMD) simulation is used for the thermal stability of the Ge (111) slabs with different thicknesses and has provided new knowledge of its potential applications. To delve deeper into the properties of Ge (111) surfaces, we executed calculations for one- and two-layer Ge (111) surface slabs. The electrical conductivities of these slabs at room temperature were determined to be 966081.89 and 760157.03 Ω^{-1} m^{-1}, respectively, with a unit cell conductivity of 1.96 Ω^{-1} m^{-1}. These findings align with actual experimental data. Notably, the electrical conductivity of the single-layer Ge (111) surface exceeded that of intrinsic Ge by 100,000 times, heralding intriguing potential for including Ge surfaces in future device applications.

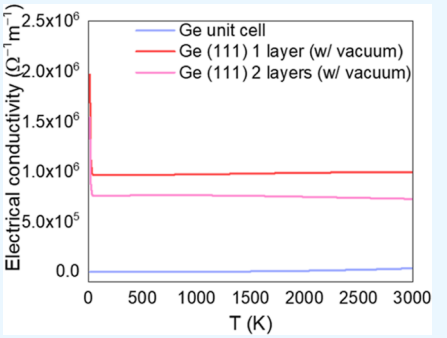

INTRODUCTION

The surface region of a semiconductor material significantly influences its interaction within a device. Consequently, surface properties can impact semiconductor devices' performance and reliability using field-effect transistors,[1,2] solar cells,[3,4] and light-emitting diodes.[5,6] Hence, a comprehensive understanding of semiconductors' surface properties and behavior is paramount to optimizing their performance and harnessing them for novel applications. The advent of advanced calculation methodologies, such as density functional theory (DFT)[7−11] and ab initio molecular dynamics (AIMD),[12−16] has empowered researchers to explore the electronic and vibrational properties of semiconductor surfaces at an atomic scale. This capability offers invaluable insights into surface phenomena.

Germanium, a group IV element, shares the sp^3 hybridization orbital characteristic with silicon. The valence electrons of an element are instrumental in defining its properties. While silicon forms four hybrid orbitals using one 3s-orbital and three 3p-orbitals, germanium employs one 4s-orbital and three 4p-orbitals. In 1947, Walter Brattain and John Bardeen introduced the first transistor, crafted by situating two gold foils on a germanium crystal.[17] Device development featuring germanium preceded silicon, attributed to its superior electron and hole mobility.[17] Additionally, the band gap of germanium (0.74 eV at 0 K) is narrower than silicon's (1.17 eV at 0 K). Despite these favorable properties, germanium presents certain drawbacks: it is less abundant than silicon, and its native oxide is unstable.[17] Consequently, silicon has emerged as the material of choice in the semiconductor industry.

The surface properties of silicon crystals have been extensively probed via density functional theory (DFT) calculations to discern the electron and phonon band structures.[18] These investigations revealed that a single layer of the (111) slab structure boasts an electron conductivity of 129.68 Ω^{-1} cm^{-1}, which is 3.23×10^7 times higher than the unit cell conductivity of silicon, measured at 4.01×10^{-6} Ω^{-1} cm^{-1} at 300 K.[18] Moreover, it was observed that the silicon (111) surface slab structure undergoes a bond distortion, resulting in a significant alteration in the electron band structure.[8] Experimental outcomes derived from a nanoprobe system within a scanning electron microscope (SEM) disclosed superior electrical conductivity on the {111} surface of an intrinsic silicon wafer compared to other surfaces, namely {110} and {100}.[19] In addition, *I*−*V* curve measurements conducted between {111} and {110} surfaces exhibited a pronounced surface diode effect.[19] These findings furnish valuable insights into the surface properties of silicon crystals, thereby offering promising implications for their potential utilization in electronic devices.

The surface effect on germanium crystals represents a research area necessitating further exploration, potentially yielding results akin to those observed for silicon. Earlier studies have indicated that the germanium (111) surface slab structure undergoes a bond-distorting phenomenon as per density functional theory (DFT) calculations.[9] Moreover, the {111} surface of intrinsic germanium wafers exhibit superior electrical conductivity compared to other surfaces, as evidenced by nanoprobe measurements within a scanning electron micro-

Received: May 9, 2023
Accepted: May 25, 2023
Published: June 7, 2023

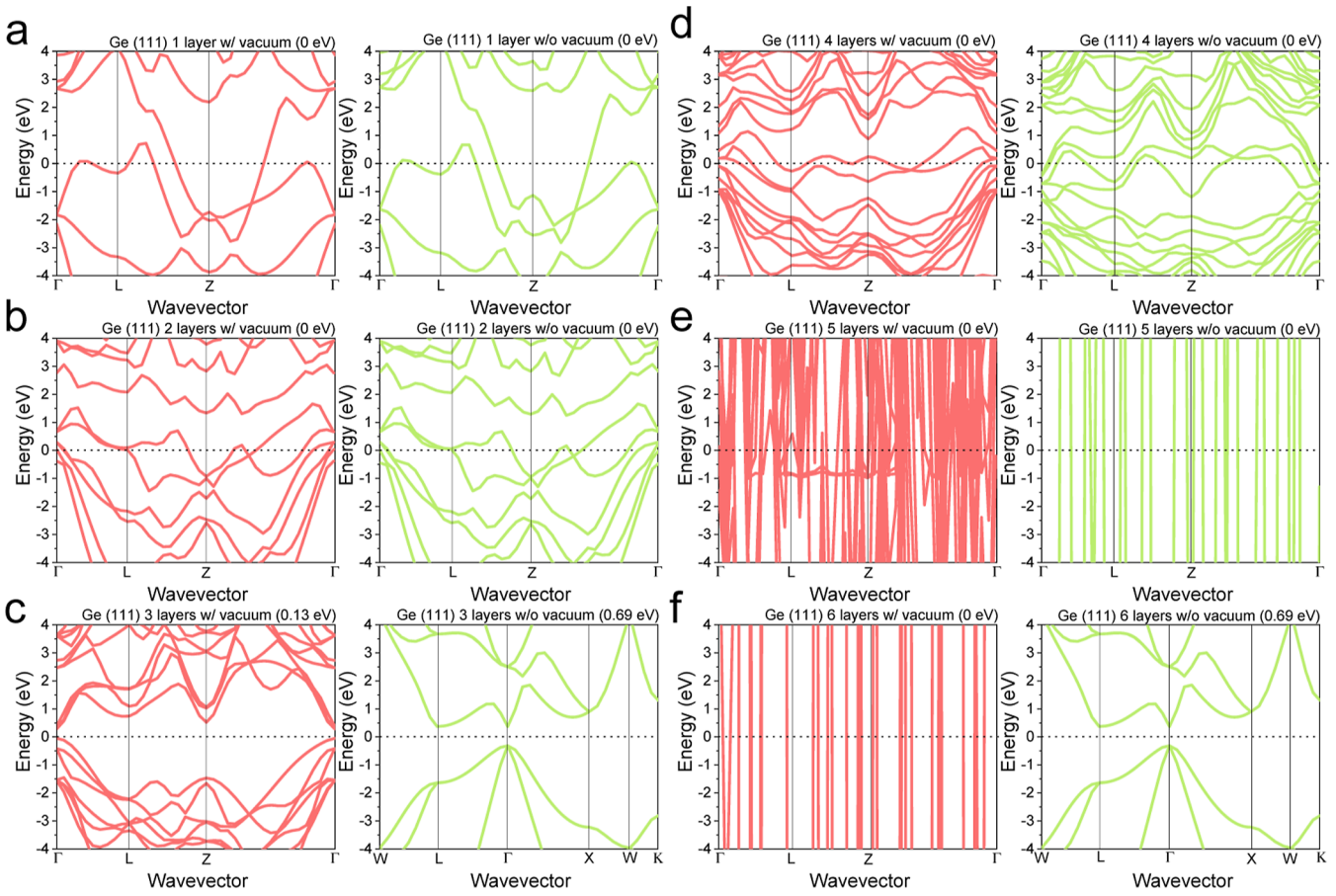

Figure 1. Band structure and electron density of states of germanium (111) slabs with and without a 0.327 nm vacuum. (a) One layer of germanium (111) slab. (b) Two layers of germanium (111) slab. (c) Three layers of germanium (111) slab. (d) Four layers of germanium (111) slab. (e) Five layers of germanium (111) slab. (f) Six layers of germanium (111) slab.

scope (SEM).[20] A surface diode effect has also been identified. Despite these findings, a comprehensive understanding of the properties of the germanium (111) surface structure remains elusive, given the absence of reported data on the electrical conductivity of the (111) germanium surface.

This study employed DFT calculations to discern the electron and phonon band structures of germanium (111) slab structures, followed by a discussion on the electrical conductivity and the dynamic stability of the surface structure. As a result, two atomic slab models of germanium (111) were established: one incorporating a vacuum layer within the slab cell and the other without. While inserting a vacuum layer in the slab cell is common among researchers for surface calculations, our findings suggest that including this vacuum layer diminishes the electrical conductivity and dynamic stability across most slab models.

As technology progresses, the demand to incorporate more transistors onto a single chip escalates to cater to the requirements of diverse applications. In large-scale transistors, characterized by a channel length in the μm range, electrons traverse from the source, across the gate, to the drain, primarily passing through the bulk single crystal of the wafer with only a minuscule proportion engaging the surface region. However, as transistor dimensions shrink, yielding a channel length of merely a few nanometers, the channel beneath the gate encompasses a more substantial segment of the surface region. Consequently, the surface effect plays a considerably more significant role in influencing the electrical behavior of the channel in these tiny transistors. This study delves into the surface effect on the electrical conductivity of the germanium (111) crystal surface, providing critical insights that could inform the development of future ultra-compact germanium transistors.

RESULTS AND DISCUSSION

Germanium is a semiconductor material with a band gap of 0.74 eV at 0 K. For this study, a germanium unit cell (as illustrated in Figure S1a) was utilized to calculate the electron band structure via DFT. As depicted in Figure S1b, the band gap of the germanium unit cell could be computed and tuned to match the experimentally determined value of 0.74 eV. The DFT calculations were performed at a base temperature of 0 K, with the electronic structures presented in Figure S1b reflecting the electron state conditions specific to germanium. Our research indicates that MBJLDA may be an appropriate functional for germanium, in line with the strong correlation approach LSDA + U. In addition, the discrepancy between the Coulomb and exchange parameters is noted to be 0.6 eV for germanium electron band structure calculations and related structure predictions.

The germanium unit cell's phonon band structure and AIMD were computed, with results in Figure S1c,d, respectively. These findings contribute to further discussions regarding the stability of the germanium unit cell and the related (111) slab structure. Furthermore, as germanium possesses both a stable crystal structure and dynamic stability, the germanium unit cell data could serve as vital reference points when assessing the dynamic

https://doi.org/10.1021/acsomega.3c03191
ACS Omega 2023, 8, 22238−22244

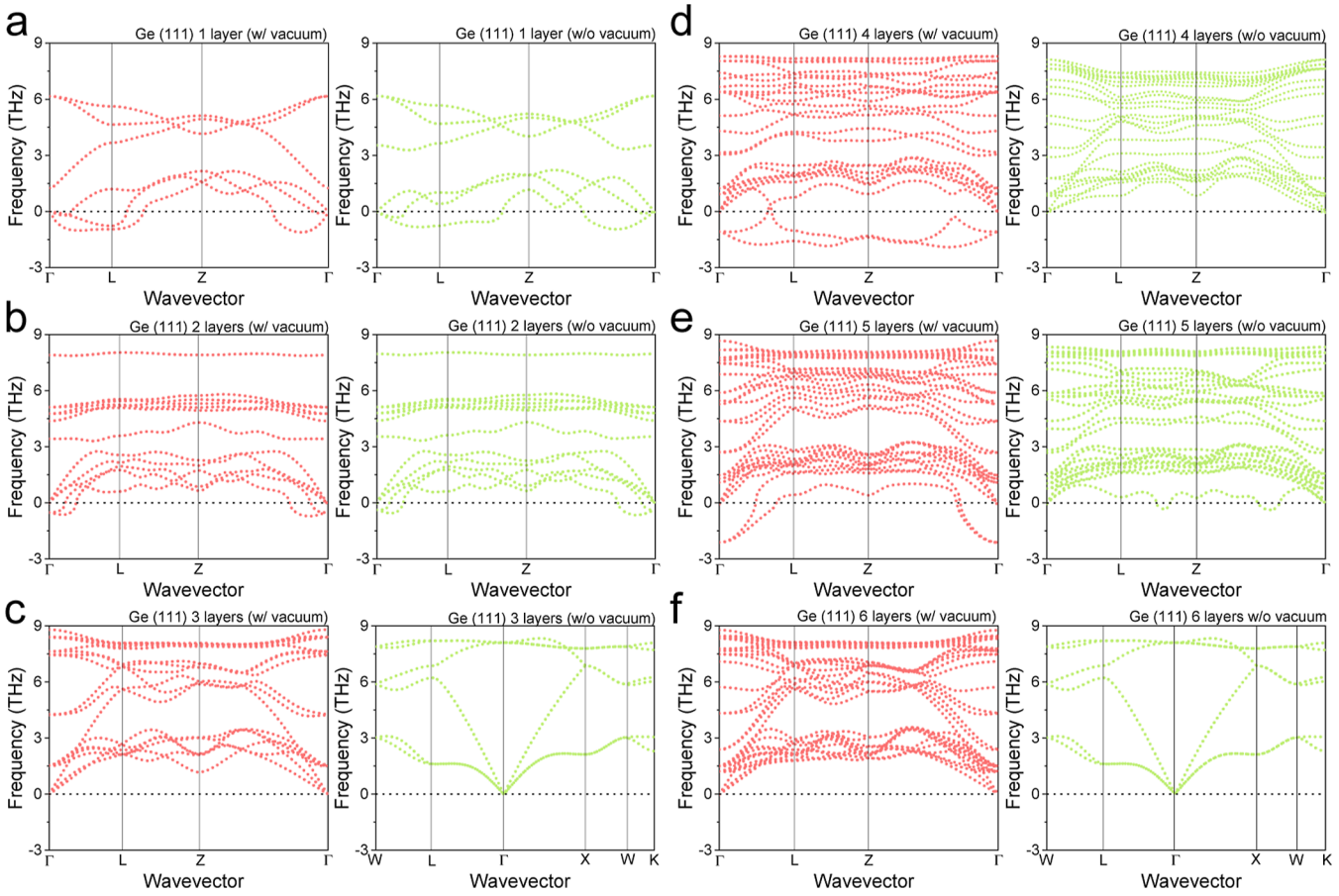

Figure 2. Phonon band structure of germanium (111) slabs with and without 0.327 nm vacuum. (a) One layer of germanium (111) slab. (b) Two layers of germanium (111) slab. (c) Three layers of germanium (111) slab. (d) Four layers of germanium (111) slab. (e) Five layers of germanium (111) slab. (f) Six layers of germanium (111) slab.

structure stability and molecular dynamic stability of germanium (111) slabs.

The atomic germanium (111) surface slab models, both with and without an inserted vacuum layer, were constructed, as shown in Figures S2a−f and S3a−f, respectively. The slabs differ in thickness, with those depicted in Figure S2a−f being thicker than those in Figure S3a−f by a margin of 0.327 nm, attributable to the inclusion of the vacuum layer. Given that the *d* spacing of germanium (111) is 0.327 nm, choosing 0.327 nm as the thickness of the vacuum layer can ensure that the atoms are isolated from the edge of the cell. The slab model containing a vacuum layer is designated as the surface slab model. In contrast, the model without the vacuum layer is classified as the crystal slab model for the germanium (111) structure.

The electron band structures for the germanium (111) surface and crystal slab models (ranging from one to six layers) were computed and are presented in Figure 1a−f. For the one-layer germanium (111) slabs depicted in Figure 1a, electrons are shown to transition seamlessly from the valence band to the conduction band at the gamma point, indicating the absence of a band gap. Consequently, both models' single-layer germanium (111) slabs can be characterized as metallic materials, with the corresponding electrical conductivity addressed in subsequent sections. In Figure 2b, a p-type band structure is formed in both models, with extra states evident above the Fermi level, albeit without an energy gap between the valence and conduction bands. However, phonon energy is required to transition electrons from the upper valence band to the conduction band.

Figure 1c shows that the three-layer germanium (111) surface slab exhibits a small band gap of 0.13 eV, whereas the crystal slab version of germanium (111) possesses a larger band gap of 0.69 eV. Examining the band structures of the three-layer germanium (111) slabs, it is apparent that the surface models diverge from the one- and two-layer slab models. In contrast, the crystal model resembles the germanium unit cell depicted in Figure S1b. In addition, the electron band structure results of the crystal models do not exhibit consistent trends, unlike those of the surface models. In Figure 1d, the four-layer germanium (111) slabs for both models display no band gap.

Furthermore, both models feature p-type electron acceptor states above the Fermi level. Electrons necessitate phonon energy for transitioning from the electron acceptor state to the conduction band. In Figure 1d, it is also noted that the crystal model harbors a greater number of electron acceptor states than the surface model.

The electron band structures in Figure 1e appear as abnormal signals, and the whole band structures are provided in Figure S4a,b. These results reveal that the five-layer slab models of germanium (111), both surface and crystal, exhibit different electron orbital conditions and are unsuitable for analysis via the MBJLDA functional. Turning to the six-layer slab models in Figure 1f, the band structure appears peculiar for the surface model, but it resembles the unit cell in Figure S1b for the crystal model. These observations suggest that calculations involving a crystal surface may be more appropriately conducted using thinner surface models with an inserted vacuum layer.

https://doi.org/10.1021/acsomega.3c03191
ACS Omega 2023, 8, 22238−22244

Conversely, slab models without a vacuum are potentially more suitable for crystal calculations, and they exhibit a triple-layer effect in the germanium (111) structures. According to the three-layer periodicity of the electron band structure, it can be inferred that the three- and six-layer germanium (111) structures are similar to the germanium unit cell. This exemplifies the triple-layer effect in slabs without a vacuum and suggests that slab models with a vacuum layer are likely better suited for surface calculations.

The phonon dispersion diagrams of the germanium (111) slabs, from one to six layers, for both surface and crystal models are computed and depicted in Figure 2a−f. As we move from one layer to three layers, the imaginary part of the phonon density of states (DOSs) for both the surface and crystal models decreases, as shown in Figure 2a−c. This indicates that the thinner the germanium (111) slab, the poorer its dynamic structural stability. For the four to six layers of germanium (111) surface and crystal slabs, it is noticeable that the four- and five-layer (111) surface slabs possess many imaginary part DOSs. In contrast, the crystal models display fewer imaginary part DOSs for the four to six layers of germanium (111) slabs. This suggests that the crystal models exhibit superior dynamic structural stability compared to the surface models.

The values of the imaginary part DOSs are tabulated in Table 1, from which two primary conclusions can be drawn. First, the one-layer germanium (111) slabs are the most dynamically unstable structures for both the surface and crystal models. Specifically, the imaginary phonon DOSs amount to 10.21% for the surface model and 12.45% for the crystal model. This reveals that a decrease in the number of layers in the slab reduces dynamic structural stability. Second, the triple layers of the surface and crystal slabs have zero (or close to zero) imaginary phonon DOSs. This indicates a triple-layer effect on the dynamic structural stability of germanium (111) slabs, suggesting that triple-layer germanium (111) slab structures have improved dynamic structural stability. AIMD can be used to calculate the molecular dynamic stability of the germanium (111) slabs, as shown in Figure 3a−f. The *y*-axis ranges are all set at 80 kJ/mol to facilitate a more straightforward comparison of energy variation over time. It is important to note that the phonon and the AIMD calculations were performed differently to demonstrate dynamic structure stability and molecular dynamic stability.

Table 1. Imaginary Part of Phonon DOS for Germanium (111) Slabs With and Without 0.327 nm Vacuum

imaginary part of phonon DOS	w/vacuum (%)	w/o vacuum (%)
Ge (111) 1 layer	10.21	12.45
Ge (111) 2 layers	3.00	2.80
Ge (111) 3 layers	0.00	0.00
Ge (111) 4 layers	8.45	0.00
Ge (111) 5 layers	1.90	0.63
Ge (111) 6 layers	0.04	0.00

For the one-layer structure models in Figure 3a, the crystal slab model displays better molecular dynamic stability than the surface slab model. However, the crystal slab model does not demonstrate a regular energy variation. This suggests that the molecular dynamics vibration of the one-layer germanium (111) crystal model is proceeding in a non-recoverable way with heat transfer. Looking at the surface and crystal slab models in Figure 3d−f, the four- to six-layer slabs exhibit molecular dynamic instability, as the energy variations are not in dynamically stable ways. However, when examining Figure 3a−f, it can be observed that only the three-layer surface slab model in Figure 3c does not show instability. All the others display signs of molecular dynamics instability under room-temperature conditions.

Figure 4a,b present the calculated electrical conductivities for the germanium unit cell, a one-layer (111) slab, and a two-layer (111) slab model. These calculations found that both one-layer and two-layer germanium (111) slab models, surface or crystal, demonstrate significantly higher electrical conductivities than the germanium unit cell. The exact electrical conductivity values can be seen in Table 2. For the surface slab models, the electrical conductivities of one-layer and two-layer germanium (111) slabs are 966081.89 and 760157.03 (Ω^{-1} m^{-1}), respectively. These values are 4.92×10^5 and 3.88×10^5 times higher than the germanium unit cell, which stands at 1.96 (Ω^{-1} m^{-1}) at room temperature. For the crystal slab models, the electrical conductivities of one-layer and two-layer germanium (111) slabs are 1140913.60 and 773358.47 (Ω^{-1} m^{-1}), respectively. These values are 5.82×10^5 and 3.95×10^5 times higher than those of the germanium unit cell, which is 1.96 (Ω^{-1} m^{-1}) at room temperature. The crystal slab models exhibit higher electrical conductivity than the surface slab models. Still, the metallic tendency of germanium (111) remains the same across all models. All the models show an electrical conductivity improvement of more than 100,000 times. This indicates that the one-layer and two-layer germanium (111) slabs are metallic materials, with or without a vacuum layer inserted.

CONCLUSIONS

Including a vacuum layer within a slab can substantially modify critical properties, including the electron band structure, phonon dispersion patterns, molecular dynamic stability, and electrical conductivity. In contrast, a germanium (111) slab devoid of a vacuum layer may lead to a three-layered arrangement. When introducing a vacuum layer to a monolayer germanium (111) slab, an amplification in dynamic structural stability is observable, counterbalanced by a decrease in molecular dynamic stability. In the molecular dynamics discussions, only the three-layer surface slab model exhibits no signs of instability. However, the surface slab models comprising three and six layers and the crystal slab models with four layers demonstrate dynamic stability. Despite the observed dynamic structural instability and molecular dynamic instability exhibited by the slab models at both 0 K and room temperature, it is noteworthy that these models consistently reveal the metallic nature of the one-layer germanium (111) surface structure. Furthermore, this specific structure exhibits exceptional electrical conductivity that surpasses that of the germanium unit cell by a factor of 100,000. Consequently, the presence and characteristics of the germanium (111) one-layer structure on the germanium (111) surface hold significant implications for the properties and performance of devices utilizing such materials.

METHOD

VASP (Vienna ab initio Simulation Package)[21−23] used and processed different exchange−correlation functionals for various purposes. The GGA-PBEsol functional [4] was used with a default plane-wave cut-off energy set at 500 eV for a Ge unit cell and slab structure optimization. The electronic iterations convergence is 1×10^{-5} eV, the Methfessel−Paxton

https://doi.org/10.1021/acsomega.3c03191
ACS Omega 2023, 8, 22238−22244

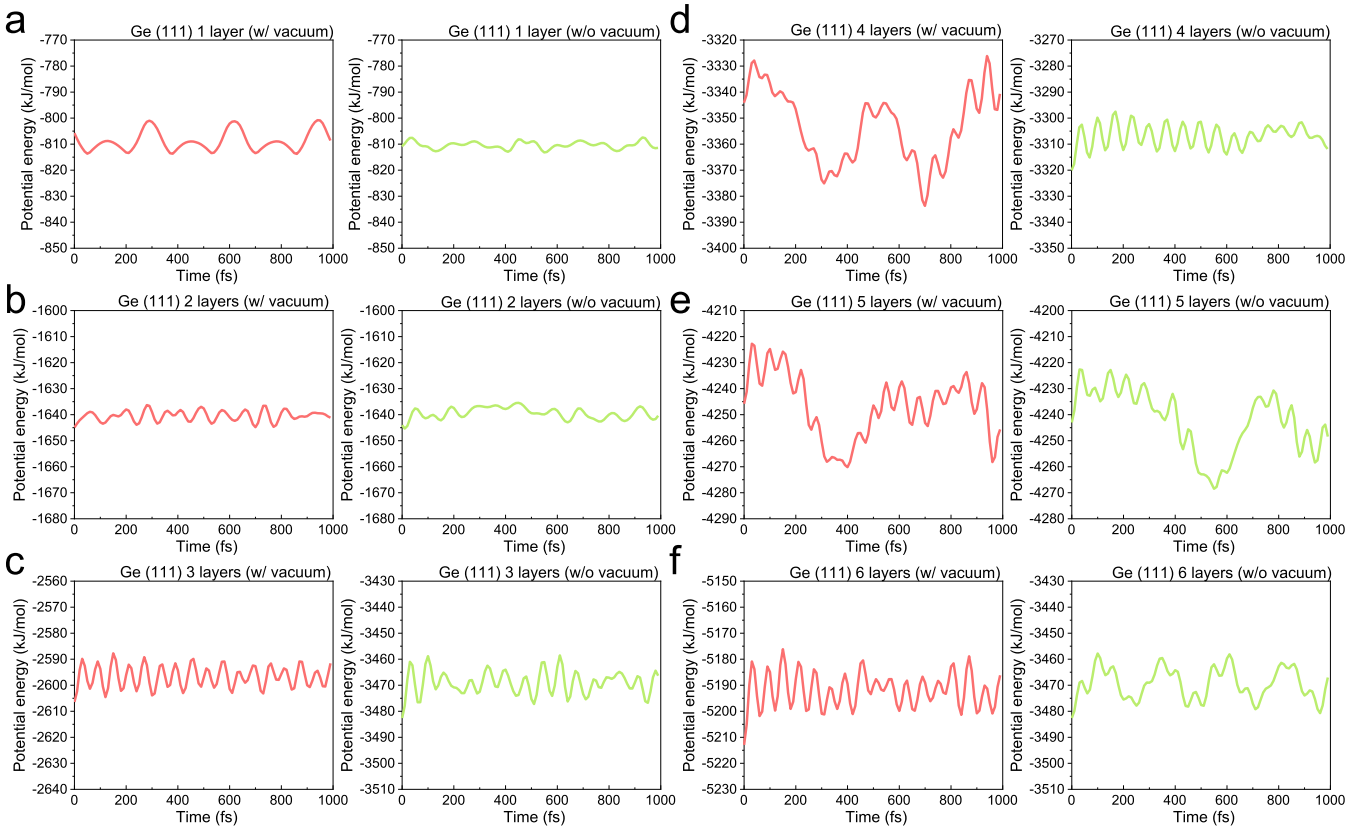

Figure 3. Molecular dynamic calculation for potential energy within 1000 fs of germanium (111) slabs with and without 0.327 nm vacuum. (a) One layer of germanium (111) slab. (b) Two layers of germanium (111) slab. (c) Three layers of germanium (111) slab. (d) Four layers of germanium (111) slab. (e) Five layers of germanium (111) slab. (f) Six layers of germanium (111) slab.

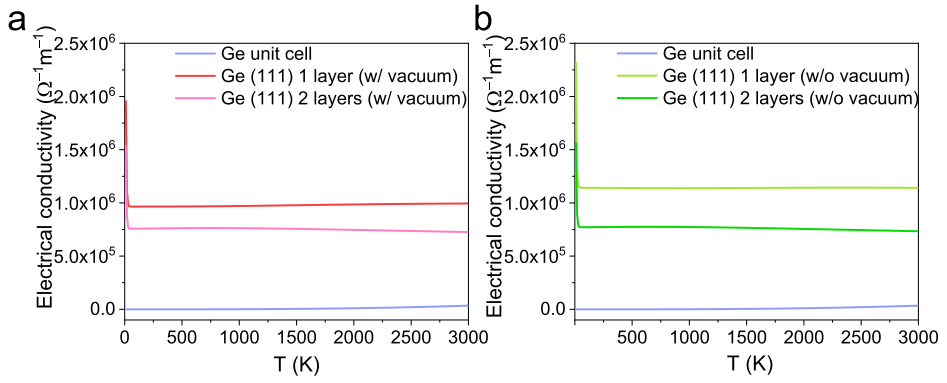

Figure 4. Electrical conductivity calculations for germanium (111) slabs and unit cell. (a)Electrical conductivity of Ge unit cell and slab models with the vacuum. (b) Electrical conductivity of Ge unit cell and slab models without vacuum.

smearing has a width of 0.2 eV, and the requested *k*-spacing is 10 × 10 × 10 mesh.

The GGA-PBE functional[24,25] processed the calculations of phonon dispersion and molecular dynamics. For the phonon dispersion diagrams, the calculations need to optimize atom positions for the supercell containing 64 atoms and run a total 2 single-point energy calculations on supercells with displaced atoms containing 64 atoms. The parameters are a default plane-wave cut-off energy of 500 eV, the electronic iterations convergence is 1×10^{-6} eV, and the *k*-spacing for non-local exchange is 10 × 10 × 10 mesh. The parameters for the molecular dynamics calculation are the microcanonical ensemble (nVE) and 298 K.

The MBJLDA *meta*-GGA density functional[26,27] processed the electron band structure calculations. The parameters are a default plane-wave cut-off energy of 500 eV, the electronic iterations convergence is 1×10^{-6} eV using the damped molecular dynamics algorithm, Gaussian smearing with a width of 0.05 eV, and the *k*-spacing is 10 × 10 × 10 mesh. As a correction for localized (strongly correlated) electrons, within the simplified LSDA + U approach, on-site Coulomb terms have been added to the Ge p orbital, and the deviation between the Coulomb parameters and the exchange parameters is 0.6 eV.

The computation of electrical conductivity was conducted by assigning 60 different chemical potentials (mu) as Fermi levels for the slabs within the band gap of germanium. These calculations utilized Boltzmann's transport theory, as imple-

https://doi.org/10.1021/acsomega.3c03191
ACS Omega 2023, 8, 22238−22244

Table 2. Electrical Conductivity Calculations of the Ge Unit Cell, Ge (111) One Layer Slabs, and Ge(111) Two Layers Slabs

T (K)	Ge unit cell (Ω^{-1} m^{-1})	Ge (111) 1 layer (w/vacuum) (Ω^{-1} m^{-1})	Ge (111) 1 layers (w/o vacuum) (Ω^{-1} m^{-1})	Ge (111) 2 layers (w/vacuum) (Ω^{-1} m^{-1})	Ge (111) 2 layers (w/o vacuum) (Ω^{-1} m^{-1})
270	0.82	965998.16	1141111.00	759790.89	773096.88
280	1.11	966026.04	1141045.30	759912.66	773183.97
290	1.49	966053.94	1140979.50	760034.79	773271.25
300	1.96	966081.89	1140913.60	760157.03	773358.47
310	2.53	966109.91	1140847.70	760279.12	773445.39
320	3.23	966138.06	1140781.80	760400.84	773531.75
330	4.06	966166.37	1140715.90	760521.94	773617.36
340	5.05	966194.90	1140650.20	760642.22	773702.00
350	6.21	966223.71	1140584.70	760761.47	773785.47
360	7.55	966252.85	1140519.50	760879.49	773867.60
370	9.09	966282.38	1140454.50	760996.1	773948.22
380	10.86	966312.38	1140389.90	761111.13	774027.16
390	12.86	966342.89	1140325.70	761224.41	774104.28
400	15.12	966374.00	1140262.00	761335.8	774179.44

mented in the BoltzTraP software. Within the initial 60 mu, 29 were selectively employed to determine electrical conductivity. All processes were carried out using the MBJLDA functional, adhering to parameter configurations identical to those in the electron band structure calculations.

■ ASSOCIATED CONTENT

Supporting Information

The Supporting Information is available free of charge at https://pubs.acs.org/doi/10.1021/acsomega.3c03191.

Additional crystal structure information (PDF).

■ AUTHOR INFORMATION

Corresponding Author

Chih Shan Tan − *Institute of Electronics, National Yang Ming Chiao Tung University, Hsinchu 30010, Taiwan;* orcid.org/0000-0001-9043-3237; Email: cstan@nycu.edu.tw

Complete contact information is available at: https://pubs.acs.org/10.1021/acsomega.3c03191

Author Contributions

C.S.T. initiated all the research ideas, performed calculations, and completed the paper writing independently.

Notes

The author declares no competing financial interest.

■ ACKNOWLEDGMENTS

This work was funded by the National Science and Technology Council of the Republic of China (Taiwan) (grants NSTC 112-2636-E-A49-003).

■ REFERENCES

(1) Fu, W.; Jiang, L.; van Geest, E. P.; Lima, L. M. C.; Schneider, G. F. Sensing at the Surface of Graphene Field-Effect Transistors. *Adv. Mater.* **2017**, *29*, 1603610. Published Online: Nov. 29, 2016

(2) She, X.-J.; Chen, C.; Divitini, G.; Zhao, B.; Li, Y.; Wang, J.; Orri, J. F.; Cui, L.; Xu, W.; Peng, J.; Wang, S.; Sadhanala, A.; Sirringhaus, H. A solvent-based surface cleaning and passivation technique for suppressing ionic defects in high-mobility perovskite field-effect transistors. *Nat. Electron.* **2020**, *3*, 694−703.

(3) Xiao, K.; Lin, R.; Han, Q.; Hou, Y.; Qin, Z.; Nguyen, H. T.; Wen, J.; Wei, M.; Yeddu, V.; Saidaminov, M. I.; Gao, Y.; Luo, X.; Wang, Y.; Gao, H.; Zhang, C.; Xu, J.; Zhu, J.; Sargent, E. H.; Tan, H. All-perovskite tandem solar cells with 24.2% certified efficiency and area over 1 cm2 using surface-anchoring zwitterionic antioxidant. *Nat. Energy* **2020**, *5*, 870−880.

(4) Wu, G.; Liang, R.; Ge, M.; Sun, G.; Zhang, Y.; Xing, G. Surface Passivation Using 2D Perovskites toward Efficient and Stable Perovskite Solar Cells. *Adv. Mater.* **2022**, *34*, No. e2105635. Published Online: Jan. 17, 2022

(5) Park, J. H.; Lee, A.-Y.; Yu, J. C.; Nam, Y. S.; Choi, Y.; Park, J.; Song, M. H. Surface Ligand Engineering for Efficient Perovskite Nanocrystal-Based Light-Emitting Diodes. *ACS Appl. Mater. Interfaces* **2019**, *11*, 8428−8435. Published Online: Feb. 15, 2019

(6) Yu, H.; Wang, H.; Zhang, T.; Yi, C.; Zheng, G.; Yin, C.; Karlsson, M.; Qin, J.; Wang, J.; Liu, X.-K.; Gao, F. Color-Stable Blue Light-Emitting Diodes Enabled by Effective Passivation of Mixed Halide Perovskites. *J. Phys. Chem. Lett.* **2021**, *12*, 6041−6047. Published Online: Jun. 24, 2021

(7) Tan, C.-S.; Huang, M. H. Surface-dependent band structure variations and bond-level deviations in Cu 2 O. *Inorg. Chem. Front.* **2021**, *8*, 4200−4208.

(8) Tan, C.-S.; Huang, M. H. Metal-like Band Structures of Ultrathin Si {111} and {112} Surface Layers Revealed through Density Functional Theory Calculations. *Chem* **2017**, *23*, 11866−11871. Published Online: Aug. 7, 2017

(9) Tan, C.-S.; Huang, M. H. Density Functional Theory Calculations Revealing Metal-like Band Structures for Ultrathin Germanium (111) and (211) Surface Layers. *Chem. Asian J.* **2018**, *13*, 1972−1976. Published Online: May. 21, 2018

(10) Tan, C.-S.; Huang, M. H. Density Functional Theory Calculations Revealing Metal-like Band Structures and Work Function Variation for Ultrathin Gallium Arsenide (111) Surface Layers. *Chem. Asian J.* **2019**, *14*, 2316−2321. Published Online: Jun. 13, 2019

(11) Tan, C.-S.; Huang, M. H. Surface-dependent band structure variations and bond deviations of GaN. *Phys. Chem. Chem. Phys.* **2022**, *24*, 9135−9140. Published Online: Apr. 20, 2022

(12) Kuo, I.-F. W.; Mundy, C. J. An ab initio molecular dynamics study of the aqueous liquid-vapor interface. *Science* **2004**, *303*, 658−660.

(13) Needels, M.; Payne, M. C.; Joannopoulos, J. D. Ab initio molecular dynamics on the Ge(100) surface. *Phys. Rev. Lett.* **1987**, *58*, 1765−1768.

(14) Novko, D.; Blanco-Rey, M.; Alducin, M.; Juaristi, J. I. Surface electron density models for accurate ab initio molecular dynamics with electronic friction. *Phys. Rev. B* **2016**, *93*, 245435.

(15) Tunega, D.; Benco, L.; Haberhauer, G.; Gerzabek, M. H.; Lischka, H. Ab Initio Molecular Dynamics Study of Adsorption Sites on the (001) Surfaces of 1:1 Dioctahedral Clay Minerals. *J. Phys. Chem. B* **2002**, *106*, 11515−11525.

(16) Lundgren, C.; Kakanakova-Georgieva, A.; Gueorguiev, G. K. A perspective on thermal stability and mechanical properties of 2D

Indium Bismide fromab initiomolecular dynamics. *Nanotechnology* **2022**, *33*, 335706. Published Online: May. 27, 2022
(17) Pillarisetty, R. Academic and industry research progress in germanium nanodevices. *Nature* **2011**, *479*, 324−328. Published Online: Nov. 16, 2011
(18) Tan, C. S. Density Functional Theory Study of Metallic Silicon (111) Plane Structures. *ACS Omega* **2022**, *7*, 5385−5392. Published Online: Feb. 2, 2022
(19) Tan, C.-S.; Hsieh, P.-L.; Chen, L.-J.; Huang, M. H. Silicon Wafers with Facet-Dependent Electrical Conductivity Properties. *Angew. Chem.* **2017**, *129*, 15541−15545.
(20) Germanium Wafers Possessing Facet-Dependent Electrical Conductivity Properties.
(21) Kresse, G.; Hafner, J. Ab initio molecular dynamics for liquid metals. *Phys. Rev. B Condens. Matter* **1993**, *47*, 558−561.
(22) Kresse, G.; Furthmüller, J. Efficient iterative schemes for ab initio total-energy calculations using a plane-wave basis set. *Phys. Rev. B Condens. Matter* **1996**, *54*, 11169−11186.
(23) Kresse, G.; Joubert, D. From ultrasoft pseudopotentials to the projector augmented-wave method. *Phys. Rev. B* **1999**, *59*, 1758−1775.
(24) Perdew, J. P.; Burke, K.; Ernzerhof, M. Generalized Gradient Approximation Made Simple. *Phys. Rev. Lett.* **1996**, *77*, 3865−3868.
(25) Perdew, J. P.; Burke, K.; Ernzerhof, M. Generalized Gradient Approximation Made Simple [Phys. Rev. Lett. 77, 3865 (1996)]. *Phys. Rev. Lett.* **1997**, *78*, 1396.
(26) Becke, A. D.; Johnson, E. R. A simple effective potential for exchange. *J. Chem. Phys.* **2006**, *124*, 221101.
(27) Tran, F.; Blaha, P. Accurate band gaps of semiconductors and insulators with a semilocal exchange-correlation potential. *Phys. Rev. Lett.* **2009**, *102*, 226401. Published Online: Jun. 3, 2009

https://doi.org/10.1021/acsomega.3c03191
ACS Omega 2023, 8, 22238−22244